Biogeosciences Discuss., 11, 16207–16226, 2014
www.biogeosciences-discuss.net/11/16207/2014/
doi:10.5194/bgd-11-16207-2014

Biogeosciences Discussions
Open Access

The vertical distribution of buoyant plastics at sea

J. Reisser[1,*], B. Slat[2,*], K. Noble[3], K. du Plessis[4], M. Epp[1], M. Proietti[5], J. de Sonneville[2], T. Becker[6], and C. Pattiaratchi[1]

[1]School of Civil, Environmental and Mining Engineering and UWA Oceans Institute, University of Western Australia, Australia
[2]The Ocean Cleanup Foundation, the Netherlands
[3]Roger Williams University, USA
[4]Pangaea Exploration, USA
[5]Instituto de Oceanografia, Universidade Federal do Rio Grande, Brazil
[6]Centre for Microscopy, Characterisation and Analysis, University of Western Australia, Australia
[*]These authors contributed equally to this work.

Received: 31 October 2014 – Accepted: 2 November 2014 – Published: 26 November 2014

Correspondence to: J. Reisser (jureisser@gmail.com)

Published by Copernicus Publications on behalf of the European Geosciences Union.

Abstract

Millimeter-sized plastics are numerically abundant and widespread across the world's ocean surface. These buoyant macroscopic particles can be mixed within the upper water column due to turbulent transport. Models indicate that the largest decrease in their concentration occurs within the first few meters of water, where subsurface observations are very scarce. By using a new type of multi-level trawl at 12 sites within the North Atlantic accumulation zone, we measured concentrations and physical properties of plastics from the air–seawater interface to a depth of 5 m, at 0.5 m intervals. Our results show that plastic concentrations drop exponentially with water depth, but decay rates decrease with increasing Beaufort scale. Furthermore, smaller pieces presented lower rise velocities and were more susceptible to vertical transport. This resulted in higher depth decays of plastic mass concentration (mg m^{-3}) than numerical concentration (pieces m^{-3}). Further multi-level sampling of plastics will improve our ability to predict at-sea plastic load, size distribution, drifting pattern, and impact on marine species and habitats.

1 Introduction

Plastics pose physical and chemical threats to the oceans' ecosystem. Their widespread occurrence at the sea surface may be shifting the distribution and abundance of marine populations due to (1) enhanced ocean drift opportunities and (2) damaging effects on biota and habitats. Plastics harbour organisms – such as fouling microorganisms, invertebrates, and fish – that can widely disperse on this new type of habitat, potentially entering non-native waters (Winston et al., 1997; Barnes, 2002; Thiel and Gutow, 2005; Zettler et al., 2013; Reisser et al., 2014a). Plastic objects can also entangle or be ingested/inhaled by marine animals, leading to impacts such as starvation, death, and hepatic stress (Derraik, 2002; Browne et al., 2008; Gregory, 2009; Rochman et al., 2013; Watts et al., 2014).

Most of what is known about at-sea plastic characteristics and concentrations comes from surface net sampling, where the top few centimetres of the water column is filtered to collect plastics larger than 0.2–0.4 mm (Hidalgo-Ruz et al., 2012). Each square kilometre of the world's sea surface contains thousands of plastic pieces known as "microplastics" when smaller than 5 mm in length (Carpenter and Smith, 1972; Cózar et al., 2014). Plastic contamination is widespread across oceans, with higher contamination levels at convergence zones such as those within subtropical gyres (Carpenter and Smith, 1972; Maximenko et al., 2012; Lebreton et al., 2012; van Sebille et al., 2012; Cózar et al., 2014). Plastic pieces are mostly fragments of packaging and fishing gear made of polyethylene and polypropylene (Morét-Ferguson et al., 2010; Reisser et al., 2013). These two resins are less dense than seawater and account for approximately 62 % of the plastic volume produced each year (Andrady, 2011).

Turbulence in the upper-ocean layer can vertically mix buoyant plastic particles. It is predicted that the largest decrease in their concentration occurs over the first meters of the water column, where only a few low-resolution measurements exist (Lattin et al., 2004; Doyle et al., 2011; Kukulka et al., 2012; Isobe et al., 2014). As studying ocean turbulent transport is heavily dependent on observations (Ballent et al., 2013; D'Asaro, 2014), high-resolution multi-level plastic sampling is urgently needed. A better understanding of the vertical transport of buoyant plastics is fundamental for improving estimates of concentration, size distribution, and dispersal of plastics at the world's ocean (Kukulka et al., 2012; Reisser et al., 2013; Law et al., 2014; Isobe et al., 2014).

In this context, the present study aimed at obtaining depth profiles of plastic pollution at the top layer of the oceans (0–5 m). We performed multi-level sampling with a new type of equipment to (1) quantify the exponential decays of plastic mass and numerical concentration with depth, and (2) demonstrate how these vary with sea state. We also provide the first experimental measurements of the rise velocity of plastic pieces, evaluating its relation to the type and size of pieces.

2 Materials and methods

2.1 At-sea sampling

We conducted 12 multi-level net tows that sampled the upper 5 m of the North Atlantic accumulation zone (Law et al., 2010; Maximenko et al., 2012; Lebreton et al., 2012) during day hours, from 19 to 22 May 2014, aboard the sailing vessel Sea Dragon (Fig. 1). We used a new type of equipment composed of eleven frames with 0.5 m height × 0.3 m width fitted with 2.1 m-long 150 µm mesh polyester nets. These nets were stacked onto each other by an external frame that was dragged in the water from eight towing points, ensuring its stability and perpendicular position in relation to the sea surface, with the top net above mean water line. Tow durations ranged from 55 to 60 min and were all undertaken while the vessel was travelling at a speed of 1–1.9 knots. The captain, who has 20 years sailing experience, estimated wind speeds and sea state while the net system was towed: beaufort scale 1 ($N = 3$ tows), 3 ($N = 4$ tows), and 4 ($N = 5$ tows). After each tow, we transferred the collected contents to a 150 µm sieve and stored them in aluminium bags that were kept frozen for transportation.

2.2 Estimating depth profiles of plastic contamination

We calculated plastic numerical and mass concentrations by dividing the number of plastic pieces and total plastic mass by the volume of filtered seawater of each net sample (pieces m^{-3} and mg m^{-3}). Filtered volume was estimated using frame dimensions and readings from a mechanical flowmeter (32 cm per rotation).

Samples were washed into a clear plastic container filled with filtered seawater, and floating macroscopic plastics were organised into gridded petri dishes for counting and characterisation. The searches for plastic pieces were of at least one hour per sample, with the aid of thumb forceps, dissecting needles, magnifying glasses, and LED torches. The latter was particularly important for detecting thin transparent plastic frag-

ments, which had low detection probability when not reflecting light. Thin filaments such as textile fibres were discarded due to potential air contamination (Foekema et al., 2013). Once all plastics were counted and characterised, they were washed with deionised water, transferred to aluminium dishes, dried at 60 °C, and weighed.

To quantify the variation of plastic concentration with depth and assess the effect of changing sea state on these vertical profiles, we first divided plastic concentration of samples by their correspondent surface concentration value. We then took the average of these normalised concentrations between adjacent nets to estimate normalised plastic concentration values at: 0 m (top 2 nets), 1 m (3th and 4th nets), 2 m (5th and 6th nets), 3 m (7th and 8th nets), 4 m (9th and 10th), and 4.75 m (11th net) deep. Finally, numerical and mass concentration values from tows collected under same Beaufort scale were grouped and fitted to exponential decay models of the form $N = e^{-\lambda z}$, where N = normalised plastic concentration, z = depth, and λ = decay rate.

We also predicted plastic concentration depth profiles using the model described in Kukulka et al. (2012): $N = e^{z w_b A_0^{-1}}$, where z = depth, w_b = plastic rise velocity, and $A_0 = 1.5 u_{*w} k H_s$ with u_{*w} = frictional velocity of water, $k = 0.4$ (von Karman constant), and H_s = significant wave height. We considered $w_b = 0.0053$ (plastics' median rise velocity, as estimated in this study), $H_s = 0.1$, 0.6, or 1 m (typical wave heights experienced at Beaufort scales 1, 3, and 4, respectively), and used the wind ranges of Beaufort 1, 3, and 4 (1–3, 7–10, and 11–16 knots, respectively) to estimate u_{*w} values through the approximation proposed by Pugh (1987): $u_{*w} = 0.00012 W_{10}$, where W_{10} = ten-metre wind speed in $m s^{-1}$.

2.3 Characterising plastic length, type, resin, and rise velocity

We measured the length of all plastic pieces using a transparent ruler (0.5 mm resolution), and classified them into the following types: hard plastic – fragments of rigid plastic; sheet – fragments of thin plastic, with some degree of flexibility; line – fragments of fishing lines or nets; foam – expanded polystyrene fragments; and pellet – raw material used to produce plastic items (Fotopoulou and Karapanagioti, 2012). We also identified the resin composition of 60 pieces using Raman spectroscopy (WITec alpha 300RA+), and measured the rise velocity of 0–3 plastics from each sample collected.

Our method of rise velocity measurement is an adaptation of an experiment to examine the fall velocity of various types of sediment particles in different fluids (Allen, 1985). Firstly, we made two marks 12.5 cm from the ends of a 1 m long clear plastic tube (diameter = 40 mm). Secondly, we filled the tube with filtered seawater, capped both its ends with rubber stops, and locked it in place with a clamp. One of the tube ends was then opened, a plastic piece placed inside, the tube closed again (with no trapped air), and quickly turned upside down and locked in place with a clamp, using a spirit level to adjust its vertical position. Finally, we recorded the time taken for the plastic piece to rise from one mark to the other (distance = 75 cm) using a stopwatch. This was measured 4 times per plastic piece, and the average was used as the estimation of its rise velocity (w_b). Rise velocities of different plastic types were separately plotted against plastic lengths (l), and linear regressions of the form $w_b = al + b$ were applied to assess the effect of plastics' characteristics on its rise velocity. We also plotted the rise velocities of plastic pieces collected at different depths to visualise depth patterns.

Finally, we calculated the fractions of plastics of different size classes (0.5–1, 1.5–2, 2.5–3, 3.5–4, 4.5–5, > 5.5 mm) that were located at the sea surface (depth < 0.5 m) and in deeper layers (depth > 0.5 m) during sampling at Beaufort scales 1, 3, and 4. We calculated these fractions using all plastics collected, as well as separated by plastic type.

3 Results

3.1 Profiles of mass and numerical concentrations

Plastic numerical and mass concentrations both decreased abruptly from their peak values at the sea surface, where median values were equal to 1.69 pieces m^{-3} and 1.60 mg m^{-3} (Fig. 2). Concentration differences between surface and deeper layers were higher in terms of mass than number of particles. For instance, median mass and numerical concentrations at 0.5–1 m were respectively 13.3 and 6.5 times lower than their median plastic peaks at 0–0.5 m.

Exponential models fitted well with both numerical and mass concentrations (R^2 = 0.99–0.84), with decay rates (λ) inversely proportional to Beaufort state (Fig. 3). Numerical concentration λ went from 3.0 at Beaufort 1 (95 % confidence interval – 95 % CI = 2.56–3.45), to 1.7 at Beaufort 3 (95 % CI = 1.51–1.88), and 0.8 at Beaufort 4 (95 % CI = 0.62–0.98). Mass concentration λ went from 3.8 at Beaufort 1 (95 % CI = 3.23–4.33), to 2.4 at Beaufort 3 (95 % CI = 1.63–3.14), and 1.7 at Beaufort 4 (95 % CI = 1.50–1.94). These decay rates were relatively similar to those predicted by Kukulka's model for Beaufort 3 (2.36–3.37) and 4 (0.88–1.28), but not for Beaufort 1 (141.73–47.2492), where the statistical fit showed much smaller λ (2.56–4.33). Mass λ were higher than numerical λ in all Beaufort scales sampled, but their 95 % CI overlapped in some cases.

3.2 Lengths, types, resins and rise velocities of plastics

We counted and classified 12 751 macroscopic plastics with lengths varying from 0.5 to 207 mm (median = 1.5 mm; Fig. 4). They were mostly fragments of polyethylene (84.7 %), followed by polypropylene (15.3 %) items. Hard plastics (46.6 %) and sheets (45.4 %) were predominant, with lower presence of plastic lines (7.9 %), pellets (0.05 %) and foams (0.008 %).

Plastic rise velocity ranged from 0.001 to 0.0438 m s^{-1} (Fig. 5a). It was directly proportional to plastic length, with the slope of this linear relationship differing among types

of plastic (Fig. 5b). While both hard plastics and sheets had a slope equal to 0.002 (95 % CI = 0.0017–0.0026 and 0.0012–0.0023, respectively), plastic lines had a flatter slope of 0.00 007 (95 % CI = 0.00002–0.00013), since their rise velocity increased only slightly towards longer pieces. Rise velocities differed among sampled depths, with particles at the surface (0–0.5 m) having a wider range of values and a higher median value than pieces at deeper depths (Fig. 5c).

The vertical mixing process was size-selective, and affected the size distribution of plastics located at the sea surface (Fig. 6), with the proportion of plastics underwater generally increasing towards smaller plastic lengths. For hard plastics and sheets, this trend was observed at all Beaufort scales sampled. Plastic lines however, only displayed this trend at Beaufort 1, with different size classes showing similar and relatively high underwater proportions at Beaufort 3 and 4 (Fig. 7).

Datasets produced and analysed in this study are available at Figshare (Reisser et al., 2014b).

4 Discussion

This study describes high-resolution depth profiles of plastic concentrations, which were shown to decrease exponentially with depth, with decay rates decreasing towards stronger winds. It also provides the first measurements of the rise velocity of ocean plastics, which varies with particle size and type. Furthermore, it shows that depth profiles of plastic mass are associated with higher decay rates than depth profiles of plastic numbers. This is due to the fact that smaller/lighter plastic pieces are generally associated with lower rising velocities, being therefore more susceptible to vertical mixing.

Predictions of plastic vertical mixing are commonly used to correct numerical concentrations obtained by surface net sampling (Kukulka et al., 2012; Reisser et al., 2013; Cózar et al., 2014; Law et al., 2014). The model described in Kukulka et al. (2012) performed relatively well in estimating the total number of plastic pieces at the wind-mixed

surface layer. The major difference between this model and our observations occurred at the calmest sea state condition (Beaufort scale 1): while the model predicted that all plastics would be at the surface, we still observed some particles underwater (> 0.5 m deep). This could have been a consequence of the presence of other types of vertical flow at our sampled sites (e. g. downwelling) or the occurrence of plastics rising from deeper waters due to previous wind-driven mixing events. This difference may be better explained in the future, by increasing sampling effort at calm conditions and collecting as much oceanographic data as possible during plastic research expeditions.

Our results indicate that plastic numerical concentration decays at a lower rate than plastic mass concentration, as lighter plastics are more susceptible to vertical transport. The uncertainties related to how plastic numerical concentration translates into plastic mass concentration have already led to differences between plastic load estimates arising from different studies. Cózar et al. (2014) used a correlation based on simultaneous surface tow measurements of total mass and abundance of plastic to convert depth-integrated numerical concentrations into mass concentrations. These authors estimated that the total plastic load in the world's sea surface layer is between 7000 and 35 000 tons. On the other hand, Law et al. (2014) multiplied depth-integrated numerical concentrations by the average plastic particle mass (1.36×10^{-5} kg), and estimated that the microplastic load at the North Pacific accumulation zone alone is of at least 21 290 tons. Such differences evidence the importance of better predicting the vertical transport of ocean plastics to develop standard plastic load estimation methods. More sampling is required to better quantify both profiles of plastic mass and numerical concentration over a broader range of sea states, and then translate these observations into prediction models.

As shown here, in a previous turbulence assay (Ballent et al., 2013), and in a modelling study (Isobe et al., 2014), vertical mixing affects the size distribution of plastics floating at the surface. We observed this effect even at low winds (1 knot), when proportions of plastics mixed into deeper waters were still increasing towards smaller particle sizes. This observation has implications for studies assessing size distribution of

plastics using surface sampling devices. Cózar et al. (2014) quantified the size distribution of plastics from worldwide sampling locations and concluded that there are major losses of small plastics from the sea surface. Here we show that at least a fraction of this "missing" plastic could be just under their sampled surface layer (0–0.5 m). For instance, 20 % of 0.5–1 mm, 13 % of 1.5–2 mm, and 8 % of 2.5–3 mm long plastics were between 0.5 and 5 m deep during our Beaufort scale 1 net tows. More at-sea and experimental work is required to quantify this effect and estimate depth-integrated size distribution of buoyant plastics drifting at sea.

The vertical mixing of buoyant plastics also affects the horizontal drifting patterns and ecological impacts of plastic pollution. For instance, larger pieces of plastic coming from land-based sources may stay trapped near the shore until further fragmentation, due to a combination of their high buoyancy and the effect of Stokes drift produced by waves parallel to coastlines (Isobe et al., 2014). Furthermore, the vertical distribution of quantities and sizes of plastics will affect how plastic contamination affects marine organisms inhabiting different depths. For instance, animals such as sea birds, turtles, and mammals (Derraik, 2002; Tourinho et al., 2010), which breath air and generally feed at the sea surface, present high plastic ingestion and entanglement rates.

Our findings show that vertical mixing affects the number, mass, and size distribution of buoyant plastics captured by surface nets, a standard equipment for at-sea plastic pollution sampling (Hidalgo-Ruz et al., 2012). Subsurface samples are still scarce and the processes influencing distribution of plastics throughout the ocean's water column are poorly understood. Further multi-level plastic sampling across a broader range of sea states is necessary for better quantifying the vertical mixing process. This will improve predictions of buoyant plastic concentration levels (Kukulka et al., 2012), size distributions (Cózar et al., 2014), drifting patterns (Isobe et al., 2014), and interactions with neustonic and pelagic species of the world's oceans.

Acknowledgements. We thank The Ocean Cleanup and The University of Western Australia for funding, Pangaea Exploration for sea time, and the staff and crew of our expedition: eric Loss, Shanley McEntee, Winston Ricardo, Bart Sturm, Beatrice Clyde-Smith,

Kasey Erin, Mario Merkus, Max Muller, and Jennifer Gelin. The authors also acknowledge The Ocean Cleanup volunteers who helped design, build, and test the multi-level trawl (see http://www.theoceancleanup.com for details). J. Reisser receives IPRS, UWA Completion, and CSIRO Postgraduate scholarships.

References

Allen, J.: Sink or Swim?, Physical Sedimentology, Springer, 1985.

Andrady, A. L.: Microplastics in the marine environment, Mar. Pollut. Bull., 62, 1596–1605, 2011.

Ballent, A., Pando, S., Purser, A., Juliano, M. F., and Thomsen, L.: Modelled transport of benthic marine microplastic pollution in the Nazaré Canyon, Biogeosciences, 10, 7957–7970, doi:10.5194/bg-10-7957-2013, 2013.

Barnes, D. K.: Biodiversity: invasions by marine life on plastic debris, Nature, 416, 808–809, 2002.

Browne, M. A., Dissanayake, A., Galloway, T. S., Lowe, D. M., and Thompson, R. C.: Ingested microscopic plastic translocates to the circulatory system of the mussel, *Mytilus edulis* (L.), Environ. Sci. Technol., 42, 5026–5031, 2008.

Carpenter, E. J. and Smith, K.: Plastics on the Sargasso Sea Surface, Science, 175, 1240–1241, 1972.

Cózar, A., Echevarría, F., González-Gordillo, J. I., Irigoien, X., Úbeda, B., Hernández-León, S., Palma, Á. T., Navarro, S., García-de-Lomas, J., and Ruiz, A.: Plastic debris in the open ocean, P. Natl. Acad. Sci. USA, 111, 10239–10244, 2014.

D'Asaro, E. A.: Turbulence in the upper-ocean mixed layer, Ann. Rev. Mar. Sci., 6, 101–115, 2014.

Derraik, J. G.: The pollution of the marine environment by plastic debris: a review, Mar. Pollut. Bull., 44, 842–852, 2002.

Doyle, M. J., Watson, W., Bowlin, N. M., and Sheavly, S. B.: Plastic particles in coastal pelagic ecosystems of the Northeast Pacific ocean, Mar. Environ. Res., 71, 41–52, 2011.

Foekema, E. M., De Gruijter, C., Mergia, M. T., van Franeker, J. A., Murk, A. J., and Koelmans, A. A.: Plastic in North Sea fish, Environ. Sci. Technol., 47, 8818–8824, 2013.

Fotopoulou, K. N. and Karapanagioti, H. K.: Surface properties of beached plastic pellets, Mar. Environ. Res., 81, 70–77, 2012.

Gregory, M. R.: Environmental implications of plastic debris in marine settings – entanglement, ingestion, smothering, hangers-on, hitch-hiking and alien invasions, Phil. Trans. R. Soc. B., 364, 2013–2025, 2009.

Hidalgo-Ruz, V., Gutow, L., Thompson, R. C., and Thiel, M.: Microplastics in the marine environment: a review of the methods used for identification and quantification, Environ. Sci. Technol., 46, 3060–3075, 2012.

Isobe, A., Kubo, K., Tamura, Y., Nakashima, E., and Fujii, N.: Selective transport of microplastics and mesoplastics by drifting in coastal waters, Mar. Pollut. Bull., 89, 324–330, 2014.

Kukulka, T., Proskurowski, G., Morét-Ferguson, S., Meyer, D., and Law, K.: The effect of wind mixing on the vertical distribution of buoyant plastic debris, Geophys. Res. Lett., 39, 1–6, 2012.

Lattin, G. L., Moore, C. J., Zellers, A. F., Moore, S. L., and Weisberg, S. B.: A comparison of neustonic plastic and zooplankton at different depths near the southern California shore, Mar. Pollut. Bull., 49, 291–294, 2004.

Law, K. L., Morét-Ferguson, S., Maximenko, N. A., Proskurowski, G., Peacock, E. E., Hafner, J., and Reddy, C. M.: Plastic accumulation in the North Atlantic subtropical gyre, Science, 329, 1185–1188, 2010.

Law, K. L., Moret-Ferguson, S., Goodwin, D. S., Zettler, E. R., DeForce, E., Kukulka, T., and Proskurowski, G.: Distribution of surface plastic debris in the eastern Pacific Ocean from an 11-year dataset, Environ. Sci. Technol., 48, 4732–4738, 2014.

Lebreton, L.-M., Greer, S., and Borrero, J.: Numerical modelling of floating debris in the world's oceans, Mar. Pollut. Bull., 64, 653–661, 2012.

Maximenko, N., Hafner, J., and Niiler, P.: Pathways of marine debris derived from trajectories of Lagrangian drifters, Mar. Pollut. Bull., 65, 51–62, 2012.

Morét-Ferguson, S., Law, K. L., Proskurowski, G., Murphy, E. K., Peacock, E. E., and Reddy, C. M.: The size, mass, and composition of plastic debris in the western North Atlantic Ocean, Mar. Pollut. Bull., 60, 1873–1878, 2010.

Reisser, J., Shaw, J., Wilcox, C., Hardesty, B. D., Proietti, M., Thums, M., and Pattiaratchi, C.: Marine plastic pollution in waters around Australia: characteristics, concentrations, and pathways, PLoS ONE, 8, e80466, doi:0.1371/journal.pone.0080466, 2013.

Reisser, J., Shaw, J., Hallegraeff, G., Proietti, M., Barnes, D. K., Thums, M., Wilcox, C., Hardesty, B. D., and Pattiaratchi, C.: Millimeter-sized marine plastics: a new pelagic habitat for microorganisms and invertebrates, PLoS ONE, 9, e100289, doi:10.1371/journal.pone.0100289, 2014a.

Reisser, J., Slat, B., Noble, K., du Plessis, K., Epp, M., Proietti, M., de Sonneville, J., Becker, T., and Pattiaratchi, C.: Data from "Float or dive? Vertical ditribution of buoyant plastics at sea", Figshare, 2014b.

Rochman, C. M., Hoh, E., Kurobe, T., and Teh, S.: Ingested plastic transfers hazardous chemicals to fish and induces hepatic stress, Nature, 3, 3263, doi:10.1038/srep03263, 2013.

Thiel, M. and Gutow, L.: The ecology of rafting in the marine environment. II. The rafting organisms and community, Oceanogr. Mar. Biol., 43, 279–418, 2005.

Tourinho, P. S., Ivar do Sul, J. A., and Fillmann, G.: Is marine debris ingestion still a problem for the coastal marine biota of southern Brazil?, Mar. Pollut. Bull., 60, 396–401, 2010.

van Sebille, E., England, M. H., and Froyland, G.: Origin, dynamics and evolution of ocean garbage patches from observed surface drifters, Environ. Res. Lett., 7, 044040, doi:10.1088/1748-9326/7/4/044040, 2012.

Watts, A. J., Lewis, C., Goodhead, R. M., Beckett, S. J., Moger, J., Tyler, C. R., and Galloway, T. S.: Uptake and retention of microplastics by the shore crab Carcinus maenas, Environ. Sci. Technol., 48, 8823–8830, 2014.

Winston, J. E., Gregory, M. R., and Stevens, L. M.: Encrusters, epibionts, and other biota associated with pelagic plastics: a review of biogeographical, environmental, and conservation issues, in: Marine Debris, Springer, 81–97, 1997.

Zettler, E. R., Mincer, T. J., and Amaral-Zettler, L. A.: Life in the "Plastisphere": microbial communities on plastic marine debris, Environ. Sci. Technol., 47, 7137–7146, 2013.

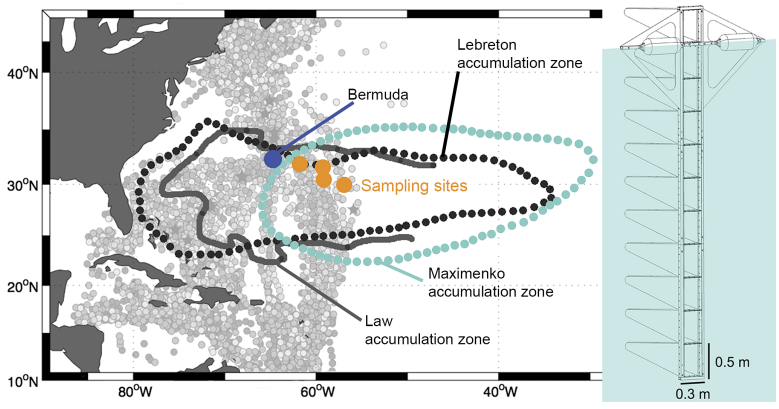

Figure 1. North Atlantic map indicating locations sampled during this study (orange dots) using the multi-level net displayed in the right panel. The map also shows the expedition departure and arrival location (Bermuda), plastic accumulation zones as predicted by ocean modelling (Lebreton et al., 2012; Maximenko et al., 2012), and a surface net tow dataset (grey dots) (Law et al., 2010).

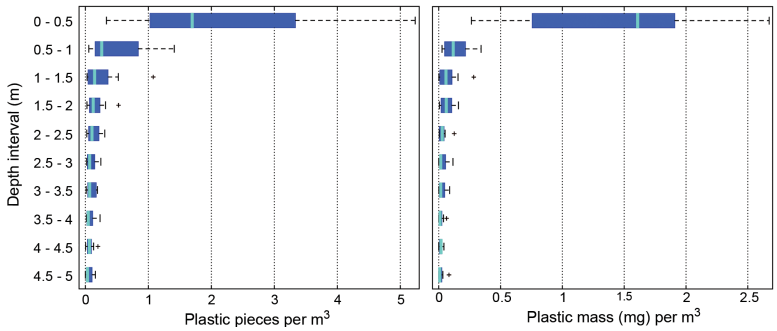

Figure 2. Boxplots of plastic numerical (left) and mass (right) concentrations at different depth intervals (N = 12 multi-level net tows). The central line is the median value, edges of the box are the 25th and 75th percentiles, whiskers extend to extreme data points not considered outliers, and outliers are plotted individually as crosses.

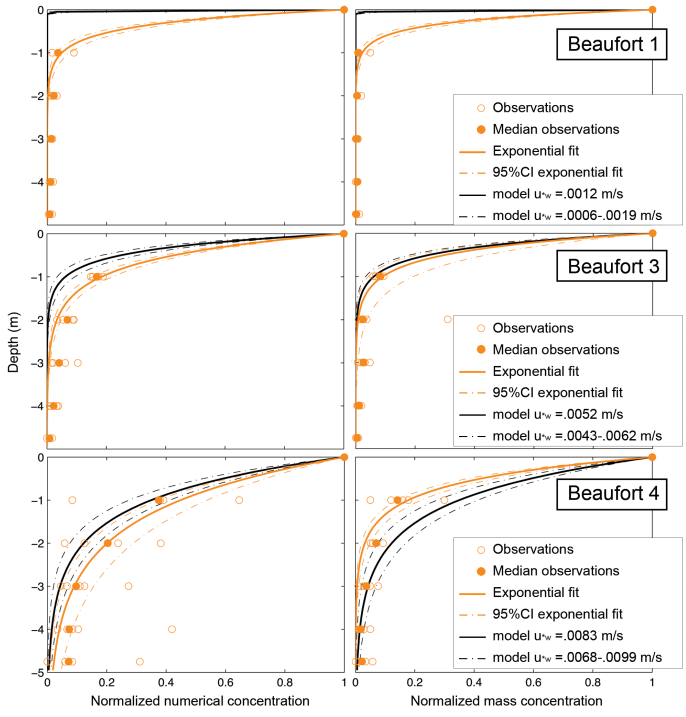

Figure 3. Depth profiles of normalized plastic numerical and mass concentrations under different Beaufort scales: 1 (N = 3 net tows; 3283 plastic pieces), 3 (N = 4 net tows; 4049 plastic pieces), and 4 (N = 5 net tows; 5419 plastic pieces). Black lines show model predictions (Kukulka et al., 2012) using median plastic rise velocity (0.0053 m s^{-1}), and the typical range of frictional velocity of water (u_{*_w}) at each of the sea states sampled.

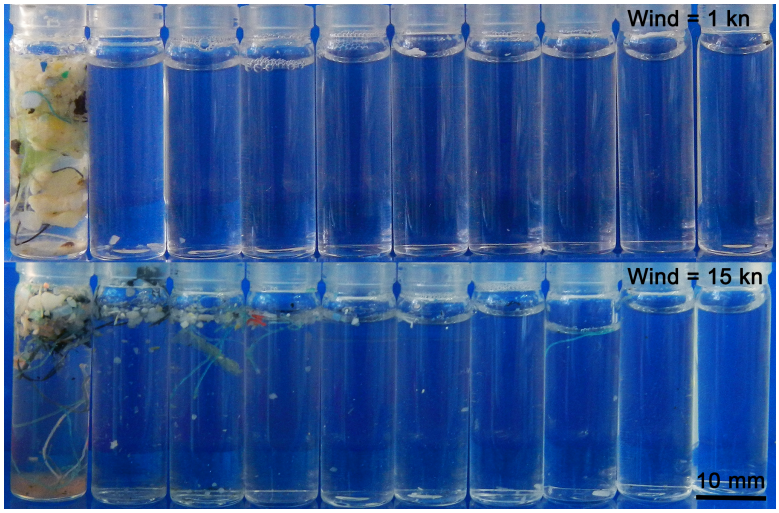

Figure 4. Glass jars with filtered water and plastic samples collected under wind speeds of 1 knot (top image) and 15 knots (bottom image). From left to right: 0–0.5, 0.5–1, 1–1.5, 1.5–2, 2–2.5, 2.5–3, 3–3.5, 3.5–4, 4–4.5, and 4.5–5 m depth intervals.

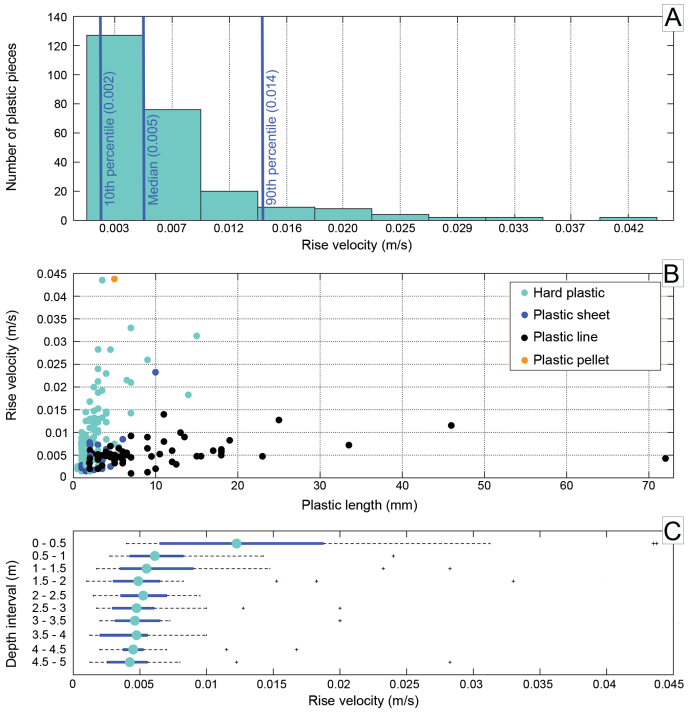

Figure 5. Histogram of rise velocity of plastics **(a)**, plots of plastic sizes x rise velocities of different types of plastic **(b)**, and boxplot of rise velocity at different depth intervals **(c)**. In **(c)**, the central dot is the median value, edges of the box are the 25th and 75th percentiles, whiskers extend to extreme data points not considered outliers, and outliers are plotted individually as crosses.

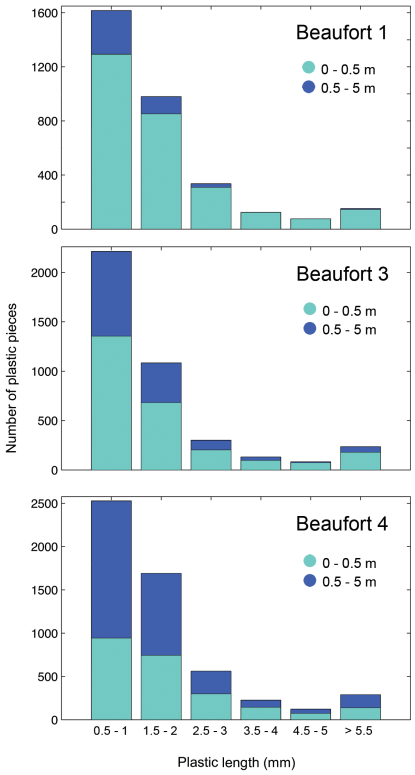

Figure 6. Size histograms of plastics collected at depths 0–0.5 and 0.5–5 m during Beaufort scale 1 (top panel), 3 (middle panel), and 4 (bottom panel).

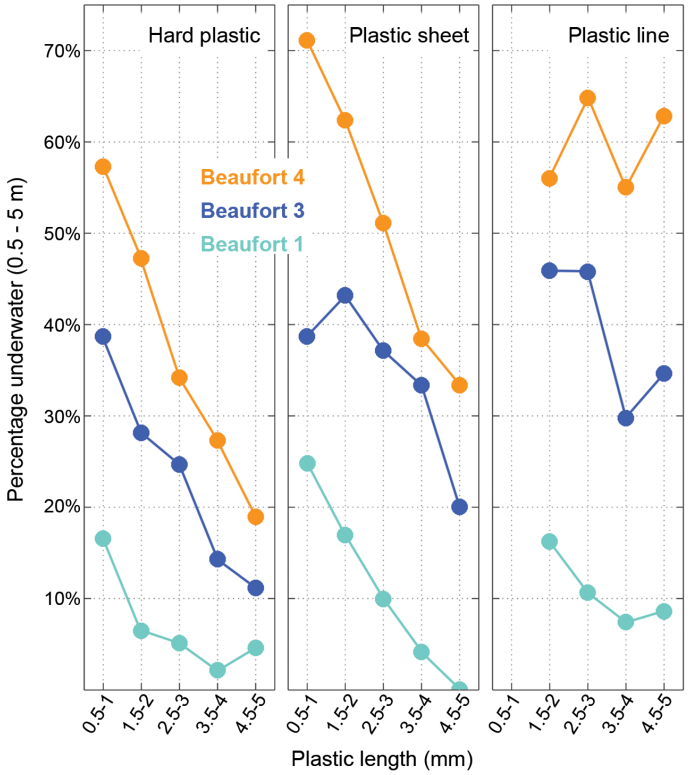

Figure 7. Percentage of plastic pieces of different types and size classes located at depths greater than 0.5 m during sampling at Beaufort scale 1, 3, and 4.